Applied Physics B (2019) 125:44
https://doi.org/10.1007/s00340-019-7157-4

Applied Physics B
Lasers and Optics

Disintegration of multiple-beam Fizeau fringes in transmission using FFT analysis

W. A. Ramadan[1] · H. H. Wahba[1,2] · M. A. El-Morsy[1,3]

Received: 12 July 2018 / Accepted: 8 February 2019 / Published online: 14 February 2019

Abstract
An investigation of fast Fourier transformation (FFT) spectrum appears from multiple-beam Fizeau fringes is presented. It is proven theoretically and demonstrated experimentally that the number of the appeared peaks is related to the interfered rays' number. In addition, a detailed interpretation of (FFT) yields from multiple-beam Fizeau fringes analyses is illustrated. This interpretation proved that every peak of the FFT spectrum represents a set of two-beam interference. Therefore, the higher order FFT peaks are not an error. It is found that the frequencies of the appeared peaks are separated by a constant increment. Therefore, when we apply the inverse fast Fourier transformation (IFFT) on a selected peak we can get a two-beam intensity distribution image with a fringe frequency depending on the peak order number. This study removes confusion and answers some important questions concerning the multiple-beam interference. The presented analysis leads to disintegrate multiple-beam interferogram to its components of two-beam interferograms. This could facilitate recovering the phase map and provides more information from one multiple-beam interferogram.

1 Introduction

The multiple-beam Fizeau fringes are being used in most accurate optical testing-based techniques [1–7]. In this kind of interference, more than two beams are superposed. Many researchers developed methods and algorithms to calculate the intensity and phase distributions of multiple-beam interference [8–12]. The accurate theories are considered when their predications and calculations meet the experimentally recorded interferograms of multiple-beam interference.

In case of two-beam interference, numerous algorithms were designed to extract the optical phase differences, with suitable accuracy, such as those algorithms based on fast Fourier transformation (FFT) and phase-shifting methods [5, 11]. On the other hand, in case of multiple-beam interference, obtaining the optical phase differences due to the occurred multiple reflections is a problematic task. One of the common methods used, to solve such a problem, was based on a phase-shifting method. It was used to extract the optical phase differences and its errors in multiple-beam Fizeau interferometer [13–17]. The phase stepping led to a significant error when a "three frames" algorithm was used instead of a "four frames" one [18]. That is besides the raised error in higher orders of FFT harmonics due to the multiple reflections. To overcome these errors, Hariharan recommended the Fourier-filtering method and he dismissed the higher orders of harmonics. Afterwards, many algorithms were proposed to reduce these errors, considering large number of frames [19, 20] and defining special filtering functions [16]. Xu et al. [14, 15] developed two methods to extract the optical phase differences considering random phase shifts in the presence of multiple-beam interference. In ref [14], a method based on FFT as well as using least squares iteration was presented. The calculations were very fast if the first harmonic of FFT was used. A suggested method based on principle component analysis; the first two components were used. Seven phase-shifted interferograms were required in the two methods. The higher orders of harmonics of Fizeau interferometry especially at very high reflectivity coefficients are still considered as a source of errors in optical phase calculations [14, 15, 18–20].

✉ W. A. Ramadan
wramadan09@gmail.com; wramadan@du.edu.eg

[1] Physics Department, Faculty of Science, Damietta University, New Damietta 34517, Egypt

[2] Physics Department, Faculty of Science, Taif University, Taif, Al-Haweiah 21974, Saudi Arabia

[3] Physics Department, College of Science and Humanitarian Studies, Prince Sattam bin Abdulaziz University, Al-kharj 11942, Saudi Arabia

Practically, the optical phase differences due to the trapped phase objects between the wedge surfaces were determined by El-Morsy et al. [21, 22]. In this case the first harmonic of FFT was used to extract the optical phase differences due to the presence of a fibrous material [22]. They neglected the higher order harmonics due to the difficulty of modeling calculation of the multiple reflected rays and its paths through the phase objects.

Recently, Ramadan presented a theory to calculate both phase and intensity distribution of Fizeau multiple-beam interference fringes [23]. In this work, the number of interfered rays was desired where rays were assumed to be transmitted through two silvered optical plates making an angle (α) in between (a wedge). In addition, the effects of wedge interferometer angle, the wedge width and the location of the formed pattern on the intensity distribution were presented. The most important result of this work was that it opened the field to review the analysis and the information that could be provided by such interferometer. Ramadan and Wahba [24] presented a development to the theory proposed in ref [23]. They estimated the intensity distribution of the interference ring fringes when light is transmitted through silvered plane-sphere optical system.

Most of the previous research work has neglected the higher orders of the resultant frequencies peaks of FFT spectra which is considered a source of errors [14, 15, 21, 22]. This besides, dealing with this kind of interference to retrieve the phase is a quite complicated task. It is obvious from this brief review that FFT spectra formation of multiple-beam Fizeau interferogram analyses is not yet well understood.

In this paper, the experimentally produced multiple-beam interference patterns as well as their corresponding estimated ones are analyzed using an algorithm based on FFT analysis. The FFT spectra of experimental and estimated patterns, when the conditions and parameters of the estimated fringes were carefully selected, were coincident. We had the facility to increase the number of the interfered rays (up to 15 rays) and monitor the related changes in FFT spectra yielded from the estimated patterns. Consequently, we were able to detect the relation between the number of the interfered rays and the FFT peaks' order. In addition, we presented an explanation of the different exist frequency peaks' orders. The higher orders of harmonics are reasonable and cannot be neglected in cases when the tiny optical phase change are occurred. Much more understanding and benefits could be obtained concerning the following: the numbers of the interfered rays, multiple-beam Fizeau fringe constitution and phase recovering for such complicated interference.

2 Construction of estimated interference pattern

In this section, we recall the theory presented by our group [23, 24]. In this theory, a ray-tracing approach has been presented to construct Fizeau fringes in transmission. It was proposed that the image plane locates at a distance L above the wedge interferometer. The wedge interferometer was consisting of two semi-silvered optical plates making an angle (α) in between. According to the geometrical path of the incident rays, each point at the image plane can be reached by a definite number of rays, see Fig. 1.

Considering different reflections and transmission made by each ray, the amplitude A_j of the ray number j reaching the point E can be written as follows [23]:

$$A_j = T \cdot R^{(j-1)}, \tag{1}$$

where

$$T = \sqrt{T_1 T_2} \text{ and } R = \sqrt{R_1 R_2}.$$

T_1 and T_2 are the transmittance of metallic layers for the upper and lower plates, respectively, while R_1 and R_2 are reflectance of the lower and upper inner plate's surfaces, respectively.

The total optical path P_j from the incident point to the point E, for the jth ray, can be obtained directly from the following relation [23]:

$$P_j = \frac{L + t_1}{\cos(2(j-1)\cdot\alpha)} + t_j \cos(\alpha) \sum_{i=1}^{2(j-1)} \frac{1}{\cos[(i-1)\alpha] \cdot \cos(i\alpha)}, \tag{2}$$

where t_1 is the wedge gap thickness traversed by the first beam. L is the distance between the upper reflecting surface and the image plane in which the interference takes place. t_j is defined as the wedge gap thickness traversed by the jth ray. More information about evaluation of t_j is given in reference [23]. Note that the incident wave is considered to be a plane wave and consequently the optical phase ϕ_j due to the optical distance traveled by the j^{th} ray can be calculated from the following relation:

$$\phi_j = \frac{2\pi}{\lambda} \cdot P_j. \tag{3}$$

Vector summation method has been used to predict the superposition between the interfered rays considering the amplitude and phase of each ray [23, 24]. The resultant amplitude η_m, due to superposition of m rays, is given as follows [23]:

$$\eta_m = \sqrt{[\eta_{(m-1)} + A_m \cos(\phi_m - \Delta_{(m-1)})]^2 + [A_m . \sin(\phi_m - \Delta_{(m-1)})]^2}, \tag{4}$$

where $m = 2$ to M, $\Delta_1 = \phi_1$ and $\eta_1 = A_1$.

Table 1 The selected parameters used to estimate multiple-beam interference fringes

Parameter	Value
Wavelength λ	532 nm
Transmittance T	15%
Reflectance R	85%
Wedge angle α	0.71°
Distance between the image plane and the interferometer upper plate L	23.25 mm
The real actual pixel size	0.146 μm

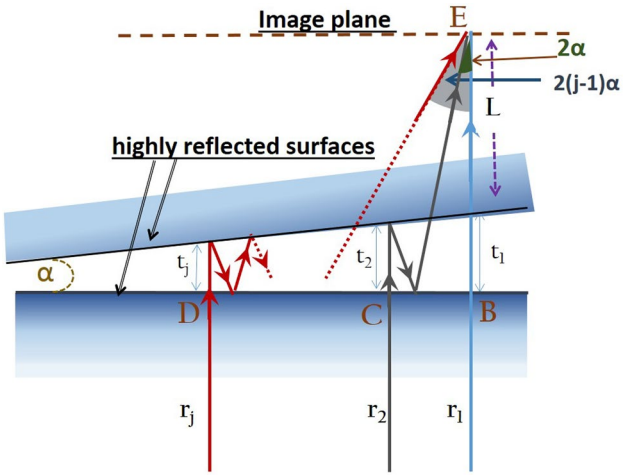

Fig. 1 A schematic diagram shows the ray tracing of the first, second and any *j*th ray. In addition, the angle between each ray and the first one is shown when the interfered rays reach a point E in the image plane locates at a height L above the upper reflected surface

M is the total number of the interfered rays. The phase angle Δ_m of the resultant interference wave of m rays is given as follows:

$$\Delta_m = \sum_{i=2}^{m} \delta_i, \tag{5}$$

where δ_m is phase difference between the resultant wave of superposition of m waves and $(m-1)$ waves and is given as follows:

$$\delta_m = \tan^{-1}\left[\frac{A_m \cdot \sin(\phi_m - \Delta_{(m-1)})}{\eta_{(m-1)} + A_m \cos(\phi_m - \Delta_{(m-1)})}\right]. \tag{6}$$

This relation was obtained using the vector summation method of waves [23, 24].

Let us clarify that the calculations will be based on the above equations which are used to estimate the multiple-beam Fizeau fringes in transmission. These fringes were formed as parallel straight lines and oriented parallel to the edge of the wedge. Therefore, the phase variation takes place as we go far from the edge of the wedge perpendicularly to the fringes' orientation. There is no phase change in the direction parallel to the edge of the wedge interferometer. In this work, a set of estimated images were constructed using a prepared programme using MATLAB environment. The parameters used to estimate these images were chosen to be quite close to the experimentally measured ones. The used parameters are listed in Table 1.

We had the facility to choose the number of the interfered rays. The desired number of interfered rays depends on the experimental interferograms, which was analyzed by FFT as explained below. Figure 2a illustrates different estimated interferograms of multiple-beam interference when we have 3, 4, 6, 8, 10, 12 and 15 interfered rays.

3 FFT analysis of the estimated pattern

The estimated patterns shown in Fig. 2a were analyzed to get their corresponding FFT spectra. We considered only the direction of phase variation so, the one-dimensional FFT spectra are listed in Fig. 2b. One can notice that the number of the peaks in the evolved spectra is proportional to the contributed number of interfered rays. It is clear from Fig. 2b that the generated peaks order number equals the number of the superposed rays. Some questions are arisen in this study; why does the number of the interfered rays equal the peak order number? Why do the powers of the different frequencies, obtained in FFT spectra, gradually decrease? Also, why the intervals between the evolved peaks are equals? That we are going to clarify in the next sections.

4 Experimental multiple-beam Fizeau interferogram in transmission

Here, we are going to generate an experimental multiple-beam Fizeau interferograms in transmission. Figure 3 shows the experimental setup used to obtain these interferograms. A solid-state continuous diode laser source of wavelength 532 nm was used. Microscope objective with a pin hole (spatial filter) and a collimating lens were aligned to get an expanded parallel beam of laser (quasi-plane wave). The wedge interferometer is consisting of two partially coated optical flats with a silver metallic layer under vacuum; the reflectance and transmittance were nearly 85% and 15%, respectively. The wedge angle between the flats was adjusted to be in the order of one degree. When the parallel rays were transmitted through the interferometer, a superposition of multiple beams took place. The generated pattern is known as a localized multiple-beam Fizeau fringes. The produced

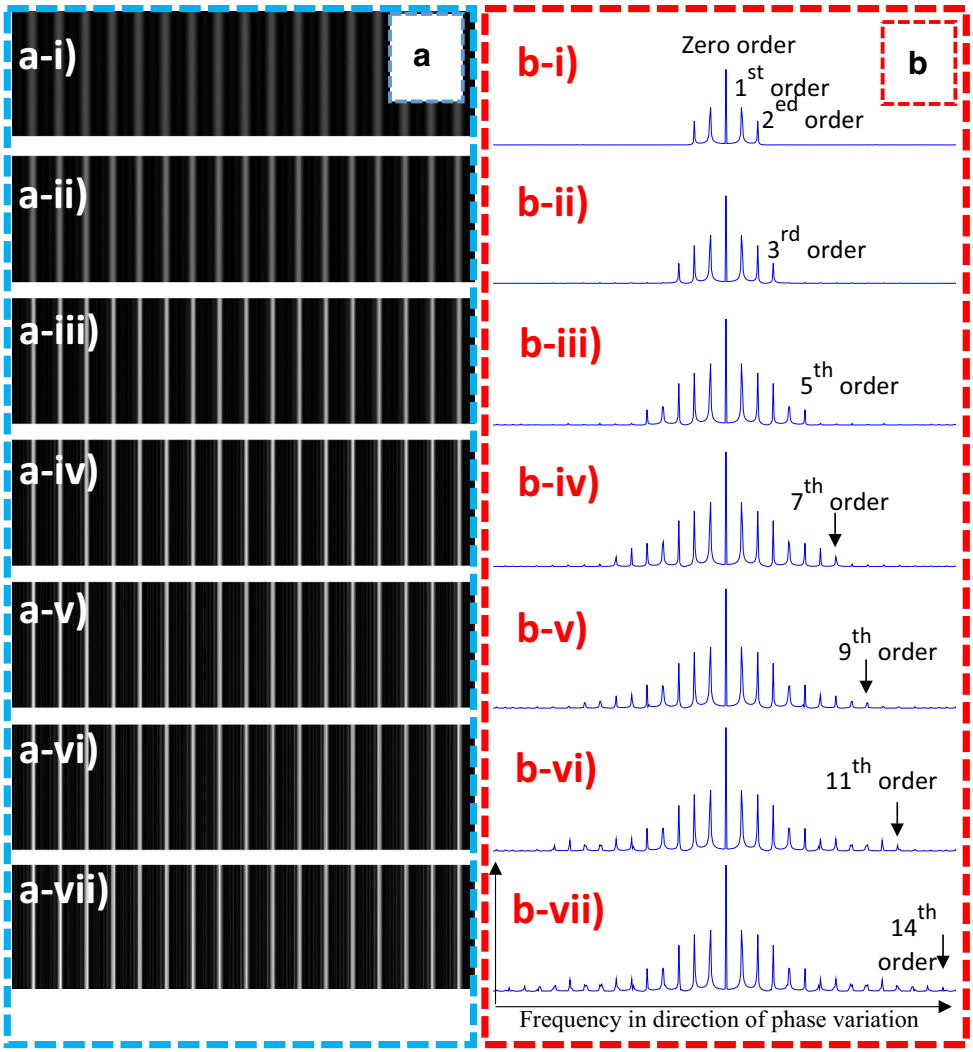

Fig. 2 **a** Set of the estimated interferograms of multiple-beam interference of 3, 4, 6, 8, 10, 12 and 15 interfered rays in images i, ii, iii, iv, v, vi and vii, respectively. **b** The corresponding FFT one-dimensional spectra illustrating the increase in number of peaks with increasing the number of the interfered rays

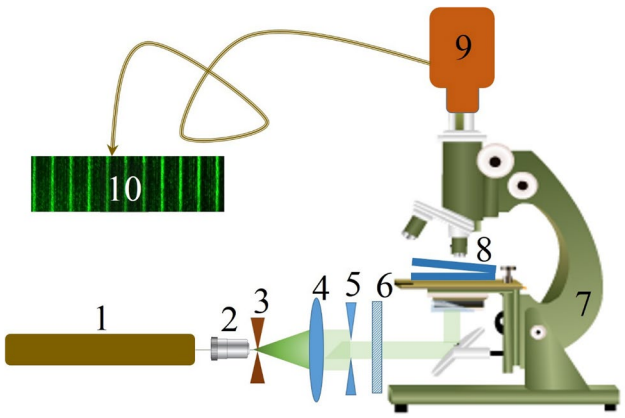

Fig. 3 A schematic diagram of multiple-beam Fizeau interferometer in transmission. 1—a solid-state continuous diode laser source of wavelength 532 nm; 2—microscope objective; 3—pin hole; 4—collimated lens; 5—diaphragm; 6—polarizer; 7—optical microscope; 8—Fizeau interferometer; 9—CCD camera; 10—recorded image

interferograms were magnified, imaged via an optical microscope and were recorded by a CCD camera.

5 FFT analysis of experimental patterns

According to the previously presented setup, we obtained an experimental interference image, shown in Fig. 4a. The FFT spectrum of the experimental image has been obtained using a prepared MATLAB programme, see Fig. 5. One can notice that the FFT spectrum of the experimental pattern provides 14 peaks around the zero order peak. Therefore, based on the previously estimated examples (see Fig. 2b), we expect to have 15 interfered rays contributed in this interference. On light of this result, we produced an estimated interference image, assuming that we have 15 interfered rays and considering similar experimental parameters, see Fig. 4b. It is quite clear how the experimental image and the estimated ones are so identical, regardless some speckle noises provided by the used laser source. The obtained FFT spectra

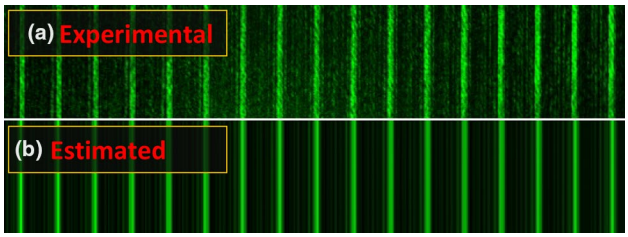

Fig. 4 Interferograms of Fizeau fringes, $\lambda = 532$ nm, for **a** experimental and **b** estimated multiple-beam Fizeau interference

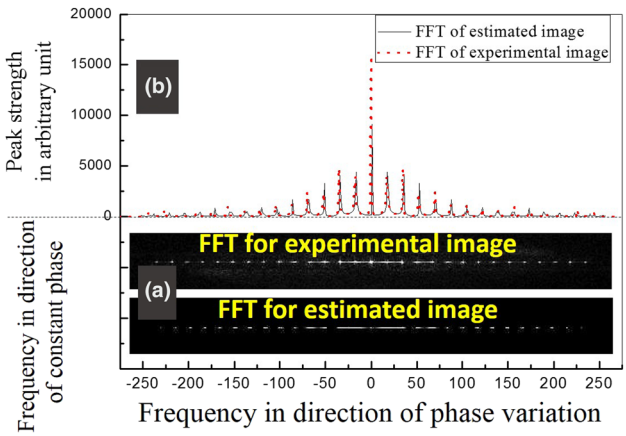

Fig. 5 **a** Two-dimensional FFT frequency spectra of the experimental and estimated images. **b** One-dimensional FFT frequency spectra (in direction of phase variation) of the experimental and estimated images which are fitted regarding the peaks numbers, peaks interspacing and the peaks height

of both experimental and estimated images are shown in Fig. 5a. In this subfigure, we can see the two-dimensional frequency images resulted from experimental and estimated interference images, respectively. In Fig. 5b, we have only the FFT in direction of phase variation showing a 15 frequency peaks including the zero order one. Moreover, the heights of the peaks also have similar behavior. A very small deviation in peak position of the higher orders between the experimental and estimated cases could be detected. In fact, we can attribute this deviation to the difference between the ideal cases of the wedge surface's flatness assumed in the estimated fringes and the real one. Anyhow, this deviation is not in our concern in this stage of the work.

6 Results and discussion

To interpret FFT spectra of the obtained multiple-beam Fizeau fringes, let us assume that we have an interference which occurs between six rays, as example, see Fig. 6. The phase difference between each two successive rays equals β. Examining the different superposition probabilities of these rays, one can realize that the interference could be occurred due to the superposition of ray no.1 with ray no.2, ray no.2 with ray no.3, ray no.3 with ray no.4 and so on. This set of two-beam interferences provides the first peak of FFT spectrum. It is clear that the optical phase difference between each pair of interfered rays, constituting this two-beam interference set, equals β. The second superposition probability could be occurring between the interference of ray no.1 with ray no. 3, ray no.2 with ray no. 4, ray no.3 with ray no. 5 and so on. This set of two-beam interference provides the second peak of FFT spectrum. The optical phase difference between each of these pairs equals the double of the phase difference of the first two-beam interference set. The third superposition could be occurred between ray no.1 with ray no.4, ray no.2 with ray no. 5, ray no.3 with ray no. 6 and so on. This set of the two-beam interference provides the third peak of FFT spectrum. One can notice that the optical phase difference of this set for each pair of interfered rays is equal to 3β.

The same interpretation can be applied for the consecutive cases of the expected superpositions. This is to realize that we can get many two-beam interference sets with increasing the peak order n. In other words, the peaks will appear on the frequency axis at separated positions, proportional to β. In addition, at the end of this treatment, it

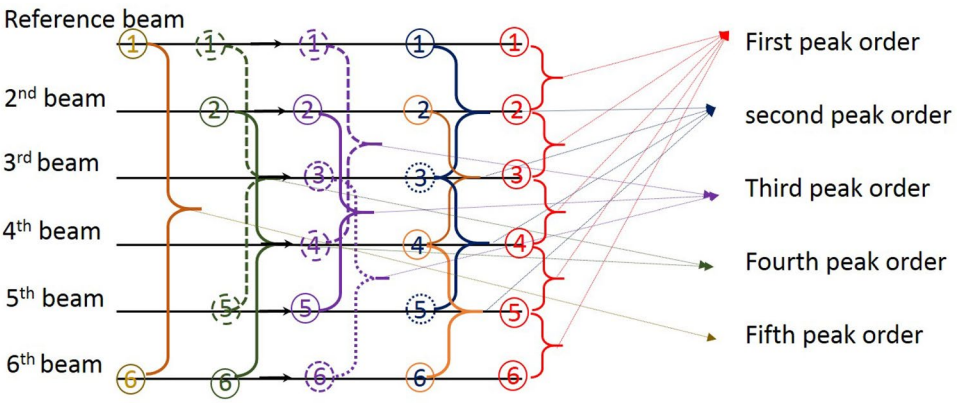

Fig. 6 A schematic diagram shows the interfered rays contributed for each order of the FFT peaks

will be evident that the total number of peaks appeared in an FFT spectrum represents the total number of the originally interfered rays. This concept could be used to retrieve the number of rays contributed in an experimental multiple-beam Fizeau interferogram. But, from a physical point of view, every one of these peaks represents a set of two-beam interferences.

Mathematically, we can consider that we have a total number of interfered rays M each one of them is indicated by a subscript j. So, the interfered rays can be represented by wave functions y_1 up to y_M. In addition, suppose that we have N total number of peaks each of them indicated by n, so n takes values from 1 to N. As it is clear from Fig. 6, each peak will represent a group of two-beam interferences. In Figures 2b and 5b, the peak height decreases with increasing the peak order n. Let W_n represent the collected superposition between the two wave functions set y_j *and* $y_{(j+n)}$ as follows:

$$W_n = \sum_{j=1}^{M} y_j + y_{(j+n)}, \qquad (j+n) \le M \tag{7}$$

where,

$$y_j = A_j \sin(\omega t + j\,\beta), \tag{8}$$

$$y_{(j+n)} = A_{(j+n)} \sin(\omega t + (j+n)\,\beta). \tag{9}$$

Considering that the amplitude of each interfered ray A_j is reduced as the number of the interfered rays increases, see Eq. (1). The relative height of the peak number n depends on the resultant intensity of the two-beam interfered sets. These resultant intensities II_n can be considered as a square of the amplitudes ξ_n obtained from the superposition of these two-beam interference set, having FFT peak number n, which can be given by

$$II_n \cong \xi_n^2 = \sum_{j=1}^{M} A_j^2 + A_{(j+n)}^2 + 2\,A_j\,A_{(j+n)} \cos(n\beta), \quad (j+n) \le M. \tag{10}$$

From Eq. (10), we can notice that there are two reasons responsible for decreasing the peak height with increasing n; the amplitude reduction of the interfered waves due to multiple reflections and decreasing of the number of summed terms. Also, regarding the frequency term in Eq. (10), it is clear that the phase constant $(n\beta)$increases linearly with n. This was expected, where the optical phase difference depends on the optical path difference which was elongated due to multiple reflections inside the wedge interferometer. We can presume that each ray exceed in optical path length by the double of the wedge gap compared with its previous one. Therefore, we have a quasi-linear increase in optical path length difference as the peak order gets higher. In other words, there is a linear increase in frequency of the two-beam interference fringes as the peak order gets higher for the same space domain. This is why we got the distance between each two successive FFT peaks almost constant.

To confirm our explanation, a single peak was selected using a defined mask, and was employed to get the IFFT for this peak. The IFFT provided an amplitude and a phase recovered from the selected peak. The obtained amplitude expresses the interference image of the two-beam interference set that was responsible for generating the selected peak. Proceeding on each peak, we got the amplitude of the two-beam interference sets responsible for different peaks. Figure 7a–d shows the amplitude images of the interference sets according to the selected order number 1, 3, 5 and 9, respectively. In Fig. 7, it is quite clear that inter-fringe spacing becomes smaller as the transformation is applied to the higher peak orders of FFT. For example, concerning Fig. 7d which represents the IFFT of the peak order number 9. It presents the sum of the following six two-beam interference cases as follows:

$$W_9 = \sum_{j=1}^{(j+9)} y_j + y_{(j+9)}, \qquad (j+9) \le 15. \tag{11}$$

Here, M (the total number of the interfered rays) equals to 15 rays. In these cases of the two-beam interference sets,

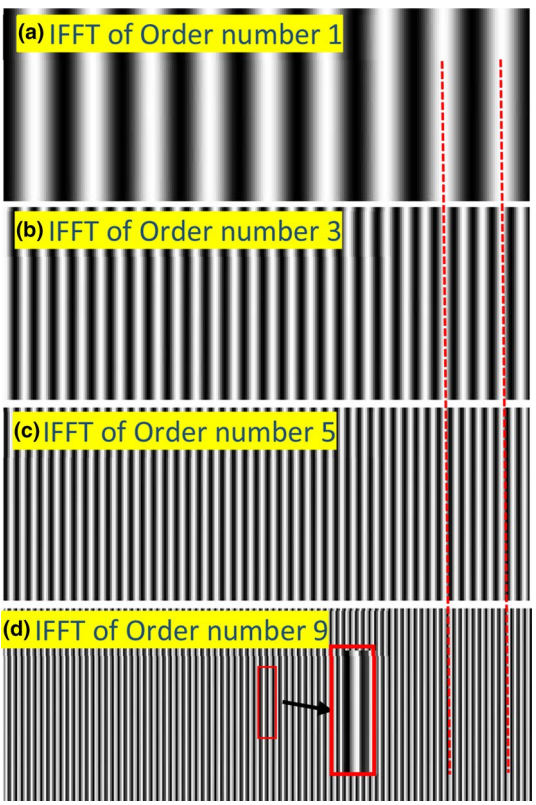

Fig. 7 Set of images presents the amplitude of the IFFT for some selected peaks of orders 1, 3, 5 and 9 from the FFT spectrum

we can notice that the object ray is reflected forward and backward (between the two interferometer surfaces) nine times more than the reference ray. Therefore, the phase difference between the interfered rays of this set equals (9β). Comparing Fig. 7a, which presents the IFFT produced from employing the first FFT peak, with Fig. 7d, one can realize that we have nine fringes in the same space of one fringe shown in Fig. 7a. The same behavior can be noticed in the IFFT images regarding the rest of the selected peaks. See Fig. 7b, c. At the end of this interpretation, we hope that we were able to answer the questions raised in "FFT analysis of the estimated pattern".

7 Conclusions

This work presents a quite good understanding of multiple-beam Fizeau interference. The ability to estimate multiple-beam interference fringe pattern demonstrated that there is a relation between the number of the FFT peaks and the number of the interfered rays. This enabled us to define, in a good perception, the number of rays forming the experimentally multiple-beam Fizeau interferogram. The novelty of this work could be summarized in the fact "each peak, yields from multiple-beam Fizeau interferogram analysis, represents a set of two-beam interferences". This gave the advantage to disintegrate the complicated multiple-beam interferograms to its original components of the two-beam interferograms. By implying IFFT, we were able to get many two-beam interferograms generated from one multiple-beam interferogram. We expect that this analysis could facilitate the phase retrieving and provide useful information utilizing any peak order separately not only the first peak order. This means that the higher peak order is not an error as was stated in previous works. The disintegration of multiple-beam Fizeau interference will open a new prospect for rethinking about benefits arising from one interferogram.

Acknowledgements The author would like to thank Prof. Dr. A. A. Hamza the leader of optics research in Mansoura and Damietta Universities for his kind encouragement. Also, many thanks to optics research group members in Damietta University for their sincere collaborations.

References

1. C.M.C.D. Hargreaves, Multiplebeam 'transmission-like' Fizeau fringes in the reflexion interference system. Nature **197**, 890 (1963)
2. L.R. Heintze, H.D. Polster, J. Vrabel, A multiple-beam interferometer for use with spherical wavefronts. Appl. Opt. **6**, 1924 (1967)
3. R. Bünnagel, H.-A. Oehring, K. Steiner, "Fizeau interferometer for measuring the flatness of optical surfaces. Appl. Opt. **7**, 331 (1968)
4. C. Roychoudhuri, in *Optical Shop Testing*, 3rd edn. by D. Malacara (Wiley, New York, 2007)
5. P. Hariharan, *Basics of interferometry*, 2nd edn. (Academic Press is an imprint of Elsevier, New York, 2007)
6. Y.P. Kumar, S. Chatterjee, Technique for the focal-length measurement of positive lenses using Fizeau interferometry. Appl. Opt. **48**, 730 (2009)
7. D.G. Abdelsalam, M.S. Shaalan, M.M. Eloker, D. Kim, Radius of curvature measurement of spherical smooth surfaces by multiple-beam interferometry in reflection. Opt. Lasers Eng. **48**, 643 (2010)
8. S. Tolansky, *Multiple beam interferometry of surfaces and films* (Clarendon Press, Oxford, 1949)
9. A.C. Hall, M.-B. Interferometry, in *Characterization of Solid Surfaces*, ed. by P.F. Kane, G.B. Larrabee (Springer US, Boston, 1974), p. 33
10. T.T. Kajava, H.M. Lauranto, A.T. Friberg, Interference pattern of the Fizeau interferometer, J. Opt. Soc. Am. A **11**, 2045 (1994)
11. D. Malacara, M. Servín, Z. Malacara, *Interferogram Analysis For Optical Testing*, 2nd edn. (CRC Press, Taylor and Francis Group, Bocca Raton, 2005)
12. E. Stoykova, Transmission of a Gaussian beam by a Fizeau interferential wedge", J. Opt. Soc. Am. A **22**, 2756 (2005)
13. B.V. Dorrı´o, J. Blanco-Garcı´a, C. Lo´pez, A.F. Doval, R. Soto, J.L. Ferna´ndez, M. Pe´rez-Amor, Phase error calculation in a Fizeau interferometer by Fourier expansion of the intensity profile", Appl. Opt. **35**, 61(1996)
14. J. Xu, Q. Xu, L. Chai, H. Peng, Algorithm for multiple-beam Fizeau interferograms with arbitrary phase shifts, Opt. Exp. **16**, 18922 (2008)
15. J. Xu, L. Sun, Y. Li, Y. Li, Principal component analysis of multiple-beam Fizeau interferograms with random phase shifts. Opt. Exp. **19**, 14464 (2011)
16. P.J. de Groot, Correlated errors in phase-shifting laser Fizeau interferometry. Appl. Opt. **53**, 4334 (2014)
17. J. Cheng, Z. Gao, Q. Yuan, K. Wang, L. Xu, Carrier squeezing interferometry with π/4 phase shift: phase extraction in the presence of multi-beam interference. Appl. Opt. **55**, 1920 (2016)
18. P. Hariharan, Digital phase-stepping interferometry: effects of multiply reflected beams. Appl. Opt. **26**, 2506 (1987)
19. Y. Surrel, Additive noise effect in digital phase detection, Appl. Opt. **36**, 271 (1997)
20. K. Hibino, Error-compensating phase measuring algorithms in a Fizeau interferometer. Opt. Rev. **6**, 529 (1999)
21. M.A. El-Morsy, T. Yatagai, A. Hamza, M.A. Mabrouk, T.Z.N. Sokkar, Multiple-beam Fizeau fringe-pattern analysis using Fourier transform method for accurate measurement of fiber refractive index profile of polymer fiber, J. Appl. Polym. Sci. **85**, 475 (2002)
22. M.A. El-Morsy, T. Yatagai, A.A. Hamza, M.A. Mabrouk, T.Z.N. Sokkar, Automatic refractive index profiling of fibers by phase analysis method using Fourier transform", Opt. Lasers Eng. **38**, 509 (2002)
23. W.A. Ramadan, Intensity distribution of Fizeau fringes in transmission with the real path of the interfered multiple-beams, Opt. Lasers in Eng. **58**, 27 (2014)
24. W.A. Ramadan, H.H. Wahba, Simulated Fizeau ring fringes in transmission through spherical and plane reflected surfaces. Appl. Phys. B **124**, 2 (2018)